New insights into the catalytic activity of gold nanoparticles for CO oxidation in electrochemical media

Paramaconi Rodriguez [a,b,c,*], Daniela Plana [b], David J. Fermin [b], Marc T.M. Koper [c,*]

[a] School of Chemistry, The University of Birmingham, Birmingham B15 2TT, UK
[b] School of Chemistry, University of Bristol, Cantocks Close, Bristol BS8 1TS, UK
[c] Leiden Institute of Chemistry, Leiden University, PO Box 9502, 2300 RA Leiden, The Netherlands

ARTICLE INFO

ABSTRACT

This study reports the interaction between metal oxides and gold in acidic media and its effect on the electrochemical oxidation of carbon monoxide. We describe the oxidation of CO in acidic media on Au nanoparticles of 3 and 7 nm on different oxide supports, diamond and carbon electrodes. In addition, the effect of a TiO_x support on Au nanoparticles was mimicked by supporting TiO_x nanoparticles on bulk gold. The comparison of these two systems strongly suggests that electronic interactions between Au and TiO_x, rather than Au nanoparticle size effects, are the driving force of the catalytic activity in Au–TiO_x.

1. Introduction

The catalytic activity of gold has attracted significant scientific attention over the years [1–9]. In gas phase, most of the work has been aimed at understanding the catalytic activity of supported nanoparticles on different metal oxides [10–21]. In particular, gold nanoparticles deposited on metal oxide supports exhibit a high catalytic activity towards CO oxidation at low temperatures [12,15,16,18,19]. Different parameters, such as the size and shape of Au clusters, the nature of the support or the preparation method, play a crucial role in influencing the catalytic activity [14,19,22,23].

In the field of electrocatalysis, the catalytic activity of bulk gold surfaces in an electrochemical environment has been investigated since the 1960s [24,25]. Two parameters that significantly influence the catalytic activity of gold in electrochemical media are the surface structure [26–31] and particularly the pH of the electrolyte [6,28–30,32,33]. Based on experimental evidence and DFT calculations, we have recently proposed a reaction mechanism for CO oxidation in which the adsorbed carbon monoxide promotes the adsorption of hydroxyl molecules and thereby enhances its own oxidation [26,27,34]. The effect is particularly strong in alkaline media, where CO is irreversibly adsorbed on gold and able to promote not only its own oxidation, but also the oxidation of other organic molecules, such as methanol [35].

Surprisingly, and in contrast to gas-phase catalysis, not many studies have been performed on the effect of the support on the electrocatalytic activity of supported gold nanoparticles [36–39]. One of the more meaningful contributions was made by Hayden et al. [37,38], who studied CO electro-oxidation on gold nanoparticles on carbon and conductive titanium oxide electrodes. From these studies, the authors found that carbon-supported gold nanoparticles show similar behaviour to that of bulk gold, while gold nanoparticles supported on sub-stoichiometric titanium dioxide showed extraordinarily high activity at low overpotentials. In both cases, the catalytic activity decreased as the Au particle size decreased below 3 nm. The interpretation of the results led the authors to conclude that the effect of particle size and substrate observed on the electro-oxidation of CO can be attributed to changes in the electronic properties of the gold derived from quantum size effects [37,38,40]. In addition, the authors suggested that the electrochemical activity must be related to the activation of water either at low-coordinate sites on titania-supported particles or at the edges of the particles.

Interestingly, the onset potential (on the Reversible Hydrogen Electrode scale) and the catalytic activity reported in references [37,38] for CO electro-oxidation on Au nanoparticles on a conductive TiO_2 support in acid media are similar to those on bulk gold

* Corresponding authors. Address: School of Chemistry, The University of Birmingham, Birmingham B15 2TT, UK (P. Rodriguez).
E-mail addresses: p.b.rodriguez@bham.ac.uk (P. Rodriguez), m.koper@chem.leidenuniv.nl (M.T.M. Koper).

electrodes in alkaline media [26,27,34]; in the latter case, no oxide support is present. Intrigued by this similarity, this study aims at studying the interaction between metal oxides and gold in acidic media and its effect on the CO electro-oxidation reaction. To this end, we have studied the oxidation of CO in acidic media on Au nanoparticles of 3 and 7 nm on different oxide supports, diamond and carbon electrodes. Simultaneously, we have studied the oxidation of CO on the 'reverse' system, *i.e.* bulk Au electrodes modified with metal oxide nanoparticles and diamond particles. Comparison of these two systems allows us to conclude that it is primarily the interaction between the gold and the oxide that leads to the enhanced catalytic activity. We do not find significant evidence for supporting claims that properties such as quantisation of energy levels, particle size or structure of either the gold particles or the support are linked to the reactivity of these systems.

2. Experimental section

In order to obtain very clean and reproducible conditions, prior to each experimental session, the cell and all glassware were immersed overnight in an acidic solution of $KMnO_4$. Next, the solution was removed and the residual MnO_4^- was rinsed with a solution of H_2O_2 and sulphuric acid (3:1) and finally was thoroughly washed several times by boiling with ultra-pure water (Millipore MilliQ gradient A10 system, 18.2 $M\Omega.cm^{-1}$, 3 ppb total organic carbon).

Highly-crystalline, type IIb, high-pressure, high-temperature diamond particles (500 nm nominal size, Microdiamant AG) were treated in a hot acid bath for 30 min (9:1 H_2SO_4:HNO_3, 200 °C) in order to remove traces of sp2 carbon, as well as generate oxygen surface groups (O-diamond) [41,42]. Hydrogen terminated diamond particles (H-diamond) were obtained by subjecting the acid-treated sample to a H_2 plasma (800 W, flow rate of 500 sccm and 50 Torr for 2 min).

The gold nanoparticles were deposited on the different substrates by using thermo evaporation in a UHV system from Edwards (pressure <1 × 10^{-6} mbar). The applied current and deposition time was changed in order to control particle size. The particle size was estimated by measuring the electrochemical surface area obtained by using the charge corresponding to the AuO reduction in the clean 0.1 M $HClO_4$ supporting electrolyte. The particle size of the gold nanoparticles was also confirmed by high-resolution transmission electron microscopy (HR-TEM) of the nanoparticles deposited under the same conditions on carbon-coated Cu TEM grids. The loading of the Au nanoparticles on the different supports was estimated from the TEM images. The loading of the 3 nm gold nanoparticles was 14.3 ± 0.4 $\mu g/cm_{geo}^2$ and 14.8 ± 0.3 $\mu g/cm_{geo}^2$ for the 7 nm nanoparticles.

2.1. Electrochemical measurements

A two-compartment electrochemical cell was employed, with a gold wire as counter electrode and a reversible Hg/HgO reference electrode. All the results are presented in a reversible hydrogen electrode (RHE) scale. Electrochemical measurements were performed with an Autolab PGSTAT12. Solutions were prepared from $HClO_4$ (Suprapure, Merck) and ultra-pure water. Ar (N66) was used to deoxygenate all solutions and CO (N47) was used to dose carbon monoxide. A flattened bead-type polyoriented gold (99.99%), HOPG (SPI-Glass™ 25 Grade), and Indium Tin Oxide (ITO) coated glass (Sigma–Aldrich and Pilkington) electrodes were used as working electrodes.

Prior to each experiment, the polyoriented gold electrodes were annealed in a propane–air flame to red heat and softly quenched with ultra-pure water; the HOPG electrode was polished with 1 μm Al_2O_3 and consequently placed in an ultra-sonic bath for

10 min and rinsed with abundant ultra-pure water. ITO electrodes were used once and discarded after use.

2.2. TiO₂ and non-stoichiometric TiOₓ nanoparticle preparation

The TiO_2 nanoparticles were prepared using the cathodic corrosion method, employing the experimental setup described in ref [43,44]. In brief, 2 mm of a Ti wire of 0.1 mm diameter was immersed in a 1 M NaOH electrolyte; an AC square wave (−10 V to 0 V) vs. a Ti counter electrode was applied at a frequency of 100 Hz, until all submerged metal was converted into a white suspension of metal oxide nanoparticles. We believe that the mechanism of formation of the titanium oxides is through the chemical oxidation of the Ti nanoparticles in NaOH. Full characterisation of the resulting nanoparticles is presented in the Supporting Information. This procedure was repeated several times, maintaining the conditions of potential, frequency, and concentration constant. The suspension of the nanoparticles was centrifuged during 5 min at 2000 RPM to remove the excess electrolyte and re-dispersed in water. TEM images and energy-dispersive X-ray (EDX) analysis are shown in the Supporting Information. In order to obtain the TiO_x, part of the TiO_2 sample was treated at 492 °C, 700 watts and a H_2 pressure of 55 Torr during 5 min. MgO (99.9 % metal basis, Alfa-Aesar) was also employed in this work.

In order to conduct experiments regarding the support effect on Au nanoparticles, compact thin films of the different supports (TiO_2, TiO_x, MgO, H-diamond and O-diamond) were prepared on the top of ITO coated glass electrodes. The films were prepared by drop-casting a colloidal suspension of the respective nanoparticles, under an Ar atmosphere. The uniformity of the films was confirmed by scanning electron microscopy.

2.3. Transmission electron microscopy and scanning electron microscopy imaging

Transmission electron microscopy was performed using a JEOL JEM 1200 EX MKI instrument and image analysis software 'analySIS 3.0' by Soft Imaging Systems GmbH. Samples were prepared by drop-casting ethanol suspensions of each catalyst on carbon-coated copper grids and drying in air. Scanning electron microscopy (SEM) was carried out on a JEOL 5600LV SEM, coupled with an Oxford Instruments 'ISIS 300' system for energy-dispersive X-ray (EDX) analysis. A JEOL field emission gun SEM 6330 was also used. SEM samples were prepared by simply placing the catalysts on a carbon sticky tab on aluminium stubs.

2.4. X-ray photoelectron spectroscopy (XPS)

X-ray photoelectron spectroscopy (XPS) elemental composition of the samples was analysed using an Escalab 250 system (Thermo VG Scientific) operating under pressure of ~1 × 10^{-9} mbar. A monochromatic Al Kα X-ray source (1486.68 eV) was used.

The Au/TiOx nanoparticles were dispersed in water by placing the ITO sample-coated glass in a 10 mL vial with 5 mL of water and into an ultrasonic bath during 10 min. The samples were prepared by drying a few drops of the sample into a soft indium foil attached to a stainless steel holder using double-sided carbon adhesive tape.

The high-resolution spectra were obtained using pass energy of 20 eV and 0.1 eV increments over a binding energy range of 20–30 eV, centred on the binding energy of the electron environment being studied. The spectra recorded were an average of 5 scans. A dwell time of 20 ms was employed between each binding energy increment. All data were base-line corrected by a linear shift such that the peak maximum of the main line in the C 1s spectra

corresponds with 284.8 eV and all signals were smoothed before the peak maximum was determined.

3. Results

3.1. Electrochemical oxidation of carbon monoxide on Au nanoparticles supported on different conducting substrates

Prior to the CO oxidation measurements, the blank voltammetric profiles of the supported nanoparticles were recorded in a 0.1 M HClO$_4$ solution. As can be observed from Fig. 1A (3 nm Au nanoparticles) and 1B (7 nm Au nanoparticles), the blank voltammograms of the supported nanoparticles are in reasonable agreement with the blank voltammogram of a polycrystalline gold electrode in the same electrolyte. The blank voltammogram of a polycrystalline gold electrode shows two oxidation peaks at ca. 1.4 and 1.6 V and one reduction peak at 1.18 V. These features are associated with the formation and the removal of gold surface oxides. In the case of the supported particles, the potential window between 0 and 0.9 V is dominated by a large double-layer charging current. At higher potentials in the positive scan, the signal of gold surface oxide formation is present. The voltammetric profiles of the supported nanoparticles differ from the Au polycrystalline electrode in that the nanoparticles exhibit a single, broad oxidation wave, shifted to more positive potentials with respect to the two peaks present in the voltammetry of the polycrystalline electrode. However, it is interesting to note that the shift in the onset of the oxidation of gold with respect to the polycrystalline electrode is independent of the support. In the negative sweep, the reduction in the gold oxide appears between 1.14 V (polycrystalline electrode and Au/TiO$_2$) and 1.20 V (HOPG and TiO$_x$). The absence of the gold peak at 1.4 V in the positive sweep and the difference in the peak potential in the negative scan could be due to traces of contamination in the support materials.

Fig. 2 shows the positive- and negative-going scans of CO oxidation on the Au nanoparticles on the different supports. For a proper comparison, CO oxidation on a polycrystalline Au electrode and on Au nanoparticles supported on HOPG is included. On the Au polycrystalline electrode, the onset potential for CO oxidation is around 0.7 V. Then, a diffusion-limited current plateau is observed

up to around 1.4 V; at higher potentials, the current decreases due to the deactivation of the surface by the oxide formation [29]. The Tafel slope for CO oxidation on the Au polyoriented electrode is 118 mV. This behaviour and the Tafel value are in agreement with previous works and confirm that the solution is fully saturated with CO [27,33,45]. For 3 nm gold nanoparticles, essentially the same behaviour is observed for all support materials (HOPG, TiO$_2$ and TiO$_x$). For the 3 nm particles, the onset of CO oxidation appears ca. 150 mV more negative than in the case of the nanoparticles deposited on HOPG, followed by a continuous increase in the current with a maximum peak current at 1.5 V vs. RHE. This maximum correlates with the potential of surface oxide formation observed in the blank. The Au nanoparticles on different supports show higher Tafel slopes, between 140 and 160 mV. The higher Tafel slopes indicate that the kinetics of CO oxidation might not be controlled solely by the adsorption of hydroxyl, but also by other surface reactions.

Fig. 2 also shows that higher currents are measured in the experiments using TiO$_2$ and TiO$_x$ supports, but these result from a flaw in the cell design. Previous studies have shown that higher CO diffusion currents can be achieved if diffusion occurs not only through the solution phase, but also through the gas phase. In our experiments, we could not avoid the contribution from CO diffusion through the gas phase. However, this 'artefact' will not affect the main conclusions from this work, which focus on the onset potential values. When the 3 nm nanoparticles were deposited on the O-terminated and H-terminated diamond electrodes, the electrochemical behaviour is similar to that observed for the nanoparticles supported on HOPG; however, the onset of the CO oxidation is slightly shifted to more positive potentials (Fig. S2). The negative-going scan for the 3 nm Au nanoparticles supported on diamond and HOPG, as well as the gold polycrystalline electrode, shows similar performance to the previous results reported in the literature: an almost zero current at high potentials, followed by a sharp activation peak at 1.4 V vs. RHE. The maximum current and decay of the current at more negative potentials is independent of the support for these cases. However, larger currents are observed for the gold nanoparticles supported on TiO$_2$ and substoichiometric TiO$_x$. As in the case of the positive scan, we believe that the current densities and the near absence of the activation peak at 1.4 V in the results presented in references [37,38] for
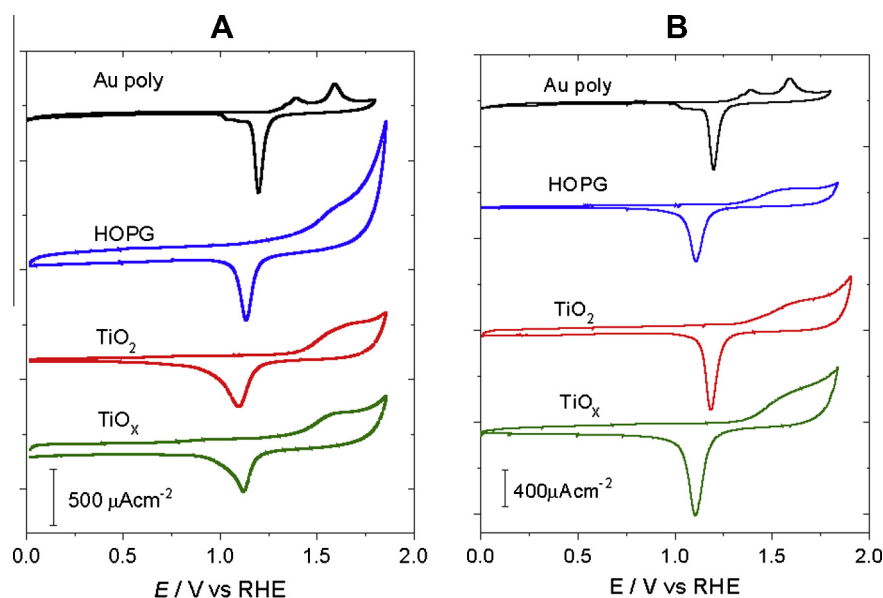

Fig. 1. Voltammetric profiles of (A) 3 nm and (B) 7 nm gold nanoparticles supported on HOPG, TiO$_x$ and TiO$_2$ as indicated in 0.1 M HClO$_4$. Scan rate 50 mV/s.
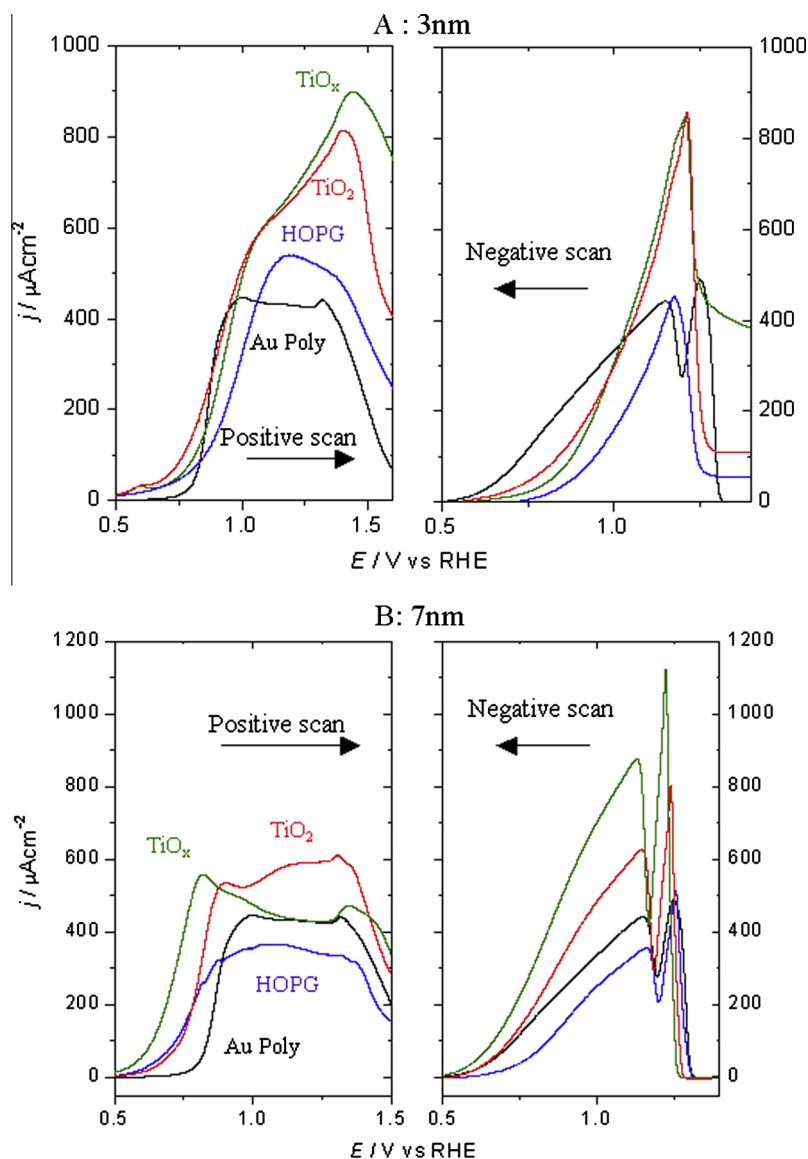
Fig. 2. Voltammetric profiles in CO-saturated 0.1 M HClO₄ of (A) 3 nm and (B) 7 nm gold nanoparticles supported on HOPG, TiO$_x$ and TiO$_2$ as indicated. The voltammetry of Au polyoriented electrode is included (–). Scan rate: 20 mV/s.

the same electrode could be related to the lower concentration of CO in their multi-array electrode configuration.

When the particle size is increased from 3 to 7 nm, the onset of CO oxidation is the same for the particles supported on HOPG. However, the CO oxidation onset potential is clearly lower than on gold polycrystalline electrodes and it is also shifted to less positive potentials on the 7 nm Au nanoparticles supported on TiO$_2$ and non-stoichiometric TiO$_2$ compared to the 3 nm particles. On the other hand, the deactivation of the gold nanoparticles due to gold oxidation takes place at similar potentials to the bulk polycrystalline gold. Interestingly, on the Ti-based supports, the continuous current increase is not observed, but instead, a semi-plateau is observed. In the negative-going scan, double reactivation peaks are observed in all cases. The different behaviours in the negative-going scan between the single reactivation peak for the 3 nm nanoparticles and the bipolar shape for the 7 nm nanoparticles are in agreement with the results reported by Hayden et al. [37,38] and can be considered a confirmation of the particle size effects.

XPS measurements have been carried out on the Au nanoparticles supported on TiO$_x$. For the sake of comparison, the XPS measurement of Au nanoparticles on carbon Vulcan was also recorded. The Au 4f lines of the Au(7 nm) nanoparticles on TiO$_x$ and the Au(3 nm) nanoparticles on TiO$_x$ have been examined in Fig. 3 . As can be seen, the binding energy of the Au 4f7/2 of the Au on carbon Vulcan (83.72 eV) is shifted 0.28 eV relative to the 84.00 eV value for metallic gold. The binding energy of the Au 4f Au(7 nm)/TiO$_x$ is shifted down up to 83.52 eV while the major shift was observed on the Au 3 nm nanoparticles supported on TiO$_x$ (83.18 eV).

3.2. Electrochemical oxidation of carbon monoxide on Au electrodes modified with metal oxide nanoparticles

In order to obtain insight about size, geometric and electronic effects, the oxidation of CO was carried out on a polycrystalline Au electrode modified with TiO$_2$, TiO$_x$, diamond and MgO nanoparticles. Figs. 4A and B show the blank voltammograms of the bare gold electrode and the same electrode modified with different loadings of TiO$_2$ and TiO$_x$ nanoparticles, respectively. The double-layer region between 0 and 0.8 V was not affected by the presence
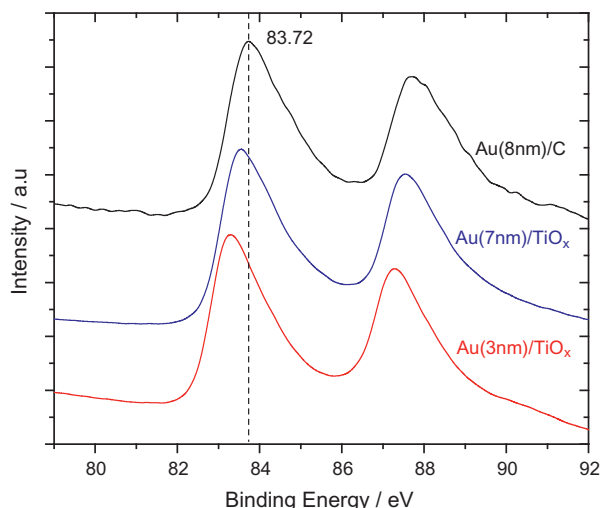
Fig. 3. Au 4f7/2 XPS spectra of the Au nanoparticles in different supports as indicated in the figure.

of the metal oxide nanoparticles (results not shown). However, gold oxide formation and reduction are strongly affected by the loading of Ti-oxide nanoparticles. In the positive scan, the peak is displaced to more positive potentials with increasing loading of the Ti nanoparticles.

A negative shift in the onset potential of CO oxidation (in the positive-going scan) was observed (Fig. 5) as a function of the surface concentration of the oxide nanoparticles. Interestingly, three peaks can be distinguished in the region between 0.2 and 0.8 V. On the bare gold electrode, the onset of CO oxidation takes place at 0.5 V, reaching a maximum current with a characteristic peak near 0.75 V. When the concentration of TiO_x nanoparticles is increased, a new peak is observed at 0.4 V which increases in current as a function of the surface concentration of nanoparticles. Concomitantly, this peak shifts towards more negative potentials. For the highest concentration of TiO_x nanoparticles, it is possible to distinguish three peaks at 0.78, 0.90 and 1.09 V vs. RHE. Three Lorentzian curves were used to fit the voltammetric profiles (Fig. S3). The decrease in the peak at 1.09 V and the increase in the peaks at 0.90 and 0.78 V as a function of the concentration of the nanoparticles suggest that the peak at lower potentials corresponds to the oxidation of CO at the interface between the Au

and the TiO_x while the peak at higher potentials corresponds to CO oxidation on the bare Au electrode. However, a more thorough analysis is required to confirm the peak assignment. Similar behaviour was observed for the TiO_2 and MgO nanoparticles as shown in Fig. 5C and Fig. 6A, respectively.

4. Discussion

The aim of this study is to elucidate three main issues in relation to gold electrocatalysis: (1) the particle size dependence of the catalytic activity of Au, (2) the role of the Au-oxide-electrolyte interface and (3) the potential impact of an electronic interactions between Au particles and the oxide material.

The enhanced activity of oxide-supported Au nanoparticles for CO oxidation in the gas phase is often proposed to arise from a direct role played by the interaction with the support and to be concentrated at the perimeter of the Au-support interface [17,18,23]. This suggestion is based on results in gas-phase conditions, where neither CO nor O_2 chemisorb on planar Au surfaces, but do chemisorb on stepped or rough Au surfaces [45–50]. However, previous studies have clearly demonstrated that the Au-support interface is not sufficient for the CO oxidation activity [51]; on relatively small particles, the amount of low coordination sites is higher than for relatively large particles, and therefore, small nanoparticles exhibit higher catalytic activity [46,48–50]. However, this assumption cannot be extrapolated to the electrochemical environment, where CO oxidation is enhanced on gold electrodes in alkaline media without a support. In an electrochemical environment, we have observed that the onset of CO oxidation takes place at lower potentials on the supported nanoparticles (3–7 nm) with respect to the gold bulk electrode, independently of the support. It has been suggested that the presence of low coordinated gold atoms must be playing a role in the enhanced catalytic activity of the supported gold nanoparticles [37,38]. However, it cannot be considered the sole driving force for CO oxidation enhancement.

Although a shift in the onset of CO oxidation was observed for Au-diamond systems a remarkable enhancement in the catalytic activity towards CO was observed for the Au-oxide systems, e.g. TiO_2, TiO_x and MgO_2. Consequently, it is important to stress the function of the perimeter interface between the Au and the oxide (either as oxide particle-Au surface or Au particles-oxide support) as a reactive site. At the Au-oxide interface, two main effects can be considered: an electronic effect and the border reaction site. In the first case, several DFT studies have tackled the interaction between
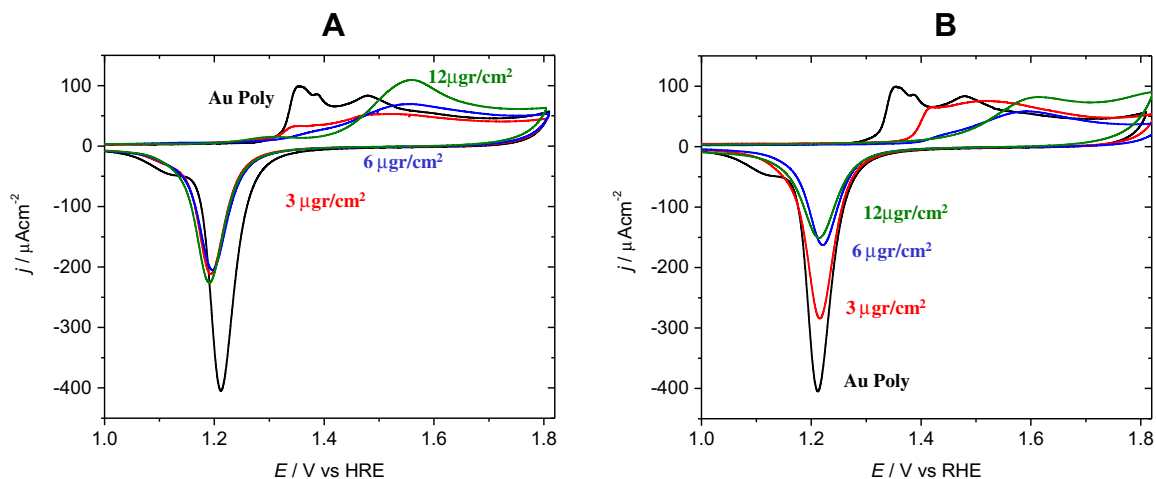

Fig. 4. Voltammetric profiles in 0.1 M $HClO_4$ of Au (polyoriented electrode) modified with different concentrations of (A) TiO_2 nanoparticles and (B) TiO_x nanoparticles. Scan rate: 50 mV/s.
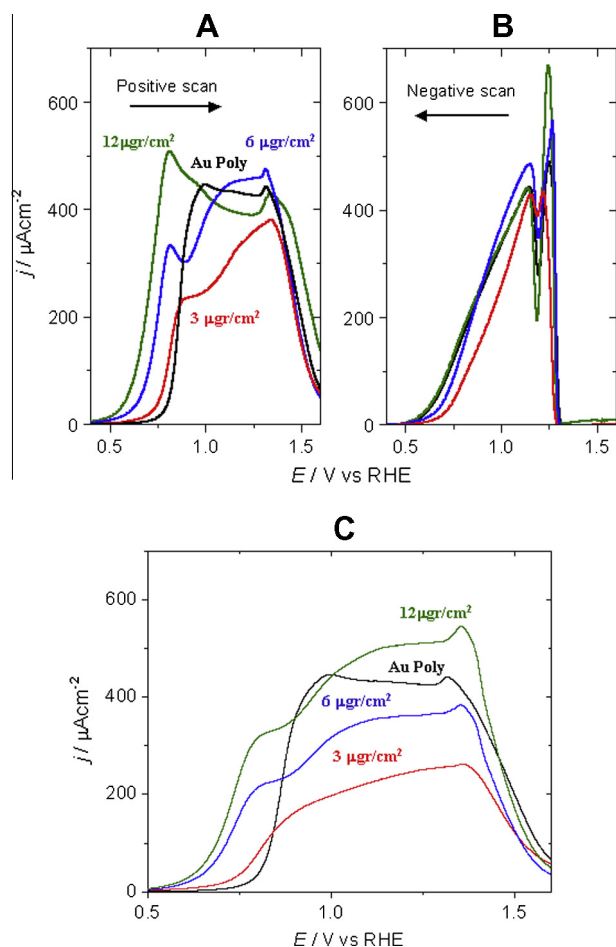
Fig. 5. Voltammetric profiles in CO-saturated 0.1 M $HClO_4$ of Au (polyoriented electrode) modified with different concentrations of TiO_2 nanoparticles (A) positive scan and (B) negative scan; and (C) TiO_x nanoparticles. Scan rate: 20 mV/s.

the Au particles and oxide supports [12,52–54]. It is agreed that Au particles bind more strongly to a defective surface than to a defect-deficient surface and that there is significant charge transfer from the support to the Au particles [53–55]. It has been accepted in gas-phase catalysis that the nature of the support directly affects the distribution and dynamics of the oxygen vacancies of the oxide and the dispersion of the Au particles, affecting the catalytic activity. However, the results of Figs. 4 and 5, where the presence of metal oxide nanoparticles was randomly supported on the bulk gold electrode (by drop-casting), demonstrate that this effect does not play a significant role in electrochemical systems.

Electron transfer from the Ti to Au nanoparticles has been probed by exciting TiO_2 nanoparticles coated with Au nanoparticles with under steady-state and laser pulse excitation [56]. In this case, it is also proposed that the presence of Au nanoparticles facilitate the migration of oxygen vacancies from the bulk to the surface of the oxide. These changes in the valence band structure presumably result from electron transfer from the surface defects on TiO_2 to the Au particles, yielding electron rich Au particles. Such a charge distribution has direct influence in dictating the energetics of the Au/TiO_2 system by shifting the Fermi level to more negative potentials. Our XPS results show negative shifts in Au 4f binding energy of the nanoparticles supported on TiO_x, with respect to the Au nanoparticles on carbon supports and bulk gold. The negative shift is more pronounced when the particle size decreases from 7 nm to 3 nm. This negative shift can be attributed to the electron transfer from the oxide to the gold. In this regard, it has been suggested that the active site for gold catalysis is anionic
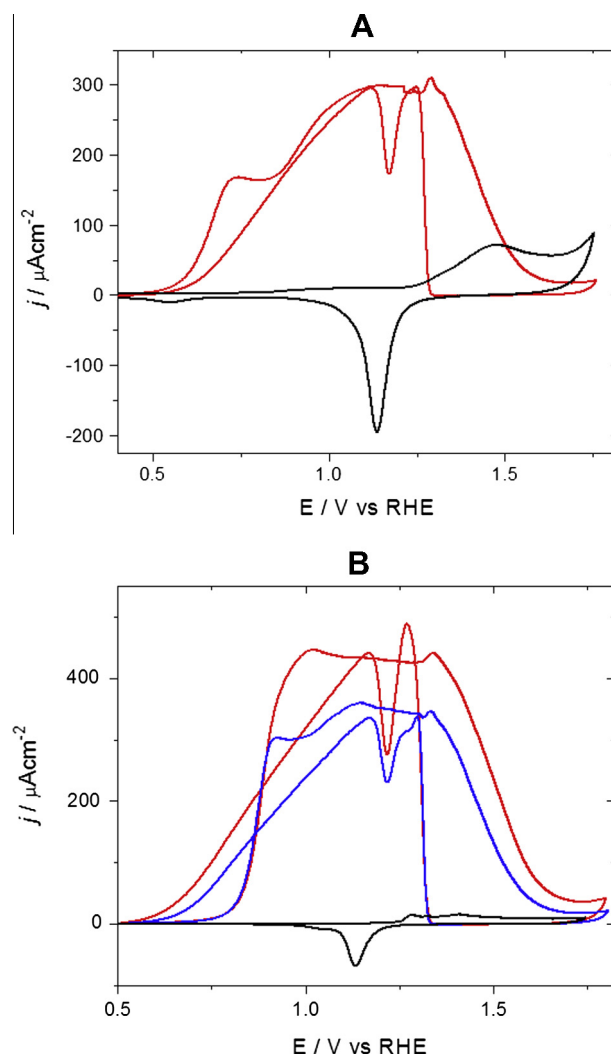

Fig. 6. (A) Voltammetric profiles of Au (polyoriented electrode) modified with MgO nanoparticles in (–) 0.1 M $HClO_4$ and (—) CO-saturated 0.1 M $HClO_4$. (B) Voltammetric profiles of Au (polyoriented electrode) in CO-saturated 0.1 M $HClO_4$ modified with (—) H-diamond and (—) O-diamond nanoparticles. Scan rate: 20 mV/s.

gold, ($Au^{\delta-}$). It is known that non-stoichiometric TiO_x behaves as an n-doped semiconductor (the Fermi level is located near the conduction band) [57], and charge transfer hence takes place between the semiconducting Au nanoparticles and the TiO_2 [58]. Such charge transfer has been also reported for the opposite case of TiO_x nanoparticles on Au(1 1 1) substrates leading to the formation of a nanosized Schottky diode [59]. Regarding the decrease in the binding energy as a function of the particle size, it is known that the binding energy Au 4f decreases with particle size, because of the increased number of surface atoms and the increase in the discrete bands with respect to the bulk Au [60]. Even though our XPS analysis suggests a higher electron density on the gold nanoparticles supported on the TiO_x, it is important to point out that the ex situ measurements do not consider the complexity of the electrochemical system. In electrochemical environment, the potential distribution at the TiO_x/electrolyte interface and the Au nanoparticles/electrolyte interface plays an important role and those are strongly dependent of surface dipoles, the water and anion adsorption and the pH. The electron transfer from the TiO_2 defects to the Au nanoparticles could be compared to the 'self-promotion mechanism' of the CO electrochemical oxidation on gold in alkaline media [26,27]. In alkaline media, the studies take place at an effectively more negative potential (vs. SHE), in comparison with acidic media; this

negative shift in the potential allows the adsorption of CO. Likewise CO induces a shift in the Fermi level of the gold, facilitating the adsorption of the hydroxyl group, which is its own oxidant.

Previous studies of the catalysed combustion of CO on monodispersed Au/MgO by temperature-programmed reaction (TPR) have revealed a partial electron transfer from the surface to the Au particle [53]. Furthermore, a direct correlation has been found between the activity of Au particles for the catalytic oxidation of CO and the concentration of F-centres at the surface of the MgO support, implying a critical role of surface F-centres in the activation of Au in Au/MgO catalysts. A decrease of 0.3 eV in the barrier for CO oxidation has been found by Sanchez et al. [12], but only when the reaction takes place at the Au atom of Au_8 cluster directly in contact with the defect site at the MgO surface.

5. Concluding remarks

As can be seen from the results presented above, CO electrochemical oxidation is strongly affected by the presence of metal oxides (TiO_2, TiO_x and MgO) in the form of either a substrate or nanoparticles. On the other hand, the presence of O- or H-terminated diamond nanoparticles does not influence CO electrochemical oxidation on gold. From the analysis of the results presented here, we can conclude the following:

1. The effect of supporting Au nanoparticles on a TiO_x support can be mimicked by supporting TiO_x nanoparticles on bulk gold. This result strongly suggests that electronic interactions are the driving force of the catalytic activity in Au–TiO_x. Similar effects were also found for the interaction between Au and conductive MgO.
2. The electrochemical oxidation of CO on gold electrodes is enhanced by an electronic effect. Such an effect can be associated to the migration of oxygen vacancies from the bulk to the surface of the oxide induced by the presence of Au nanoparticles. Such a cooperative effect between the gold nanoparticles and the oxide induces changes in the valence band structure of the Au particles by shifting the Fermi level to more negative potentials. Ex situ XPS measurements showed a higher electron density in the Au nanoparticles supported on TiO_x suggesting the presence of anionic gold ($Au^{\delta-}$) species. The catalytic activity of gold in heterogeneous catalysis has been attributed to this anionic species, however in electrochemical media other electronic effects as the potential distribution at the nanoparticles/support/electrolyte interface cannot be ruled out and the surface dipoles and pH are dominant factors of the potential distribution hence the catalytic activity.
3. It has been suggested that the metal oxides induce a negative charge in the gold nanoparticles comparable to the negative charge induced by the effectively more negative potential (SHE) of the electrodes in alkaline media. In both cases, the negative charge on the gold surface favours the co-adsorption of CO and OH, as explained by the 'self-promotion mechanism'.

Acknowledgments

Appendix A. Supplementary material

Supplementary data associated with this article can be found, in the online version, at http://dx.doi.org/10.1016/j.jcat.2013.11.020.

References

[1] M. Haruta, Catalysis: gold rush, Nature 437 (7062) (2005) 1098–1099.
[2] T. Hayashi, K. Tanaka, M. Haruta, Selective vapor-phase epoxidation of propylene over Au/TiO_2 catalysts in the presence of oxygen and hydrogen, J. Catal. 178 (2) (1998) 566–575.
[3] C.H. Christensen, J.K. Nørskov, Green gold catalysis, Science 327 (5963) (2010) 278–279.
[4] G.J. Hutchings, M. Brust, H. Schmidbaur, Gold – an introductory perspective, Chem. Soc. Rev. 37 (9) (2008) 1759–1765.
[5] A.S.K. Hashmi, G.J. Hutchings, Gold catalysis, Angew. Chem.—Int. Ed. 45 (47) (2006) 7896–7936.
[6] K. Kunimatsu et al., Infrared-spectra of carbon-monoxide adsorbed on a smooth gold electrode. 2. Emirs and polarization-modulated irras study of the adsorbed co layer in acidic and alkaline-solutions, J. Electroanal. Chem. 207 (1–2) (1986) 293–307.
[7] Y. Wang, E. Laborda, R.G. Compton, Electrochemical oxidation of nitrite: kinetic, mechanistic and analytical study by square wave voltammetry, J. Electroanal. Chem. 670 (2012) 56–61.
[8] A. Saez et al., Gold supported catalytic layer: an intermediate step between fundamental and applied fuel cell studies, Electrochim. Acta 54 (27) (2009) 7071–7077.
[9] J. Hernandez et al., Methanol oxidation on gold nanoparticles in alkaline media: unusual electrocatalytic activity, Electrochim. Acta 52 (4) (2006) 1662–1669.
[10] A.K. Santra, D.W. Goodman, Oxide-supported metal clusters: models for heterogeneous catalysts, J. Phys.—Condens. Matter 15 (2) (2003) R31–R62.
[11] J.A. Rodriguez et al., High water-gas shift activity in $TiO_2(110)$ supported Cu and Au nanoparticles: role of the oxide and metal particle size, J. Phys. Chem. C 113 (17) (2009) 7364–7370.
[12] I.N. Remediakis, N. Lopez, J.K. Norskov, CO oxidation on rutile-supported Au nanoparticles, Angew. Chem.—Int. Ed. 44 (12) (2005) 1824–1826.
[13] J.B. Park et al., High catalytic activity of Au/CeO_x/$TiO_2(110)$ controlled by the nature of the mixed-metal oxide at the nanometer level, Proc. Nat. Acad. Sci. U.S.A. 106 (13) (2009) 4975–4980.
[14] Y. Maeda et al., Size and density of Au particles deposited on TiO_2 (110)-(1x1) and cross-linked (1x2) surfaces, Surf. Sci. 562 (1–3) (2004) 1–6.
[15] A. Kolmakov, D.W. Goodman, Scanning tunneling microscopy of gold clusters on $TiO_2(110)$: CO oxidation at elevated pressures, Surf. Sci. 490 (1–2) (2001) L597–L601.
[16] G.J. Hutchings et al., Role of gold cations in the oxidation of carbon monoxide catalyzed by iron oxide-supported gold, J. Catal. 242 (1) (2006) 71–81.
[17] M. Haruta et al., Synergism in the catalysis of supported gold, Stud. Surf. Sci. Catal. 77 (1993) 45–52.
[18] M. Haruta, When gold is not noble: catalysis by nanoparticles, Chem. Rec. (New York, N.Y.) 3 (2) (2003) 75–87.
[19] M. Haruta, Catalysis of gold nanoparticles deposited on metal oxides, Cattech 6 (3) (2002) 102–115.
[20] R. Grisel et al., Catalysis by gold nanoparticles, Gold Bull. 35 (2) (2002) 39–45.
[21] M. Chen, D.W. Goodman, Catalytically active gold on ordered titania supports, Chem. Soc. Rev. 37 (9) (2008) 1860–1870.
[22] T. Ishida et al., Influence of the support and the size of gold clusters on catalytic activity for glucose oxidation, Angew. Chem.—Int. Ed. 47 (48) (2008) 9265–9268.
[23] G.J. Hutchings, M. Haruta, A golden age of catalysis: a perspective, Appl. Catal. a—Gen. 291 (1–2) (2005) 2–5.
[24] J.L. Roberts Jr., D.T. Sawyer, Electrochemical oxidation of carbon monoxide at gold electrodes, Electrochim. Acta 10 (10) (1965) 989–1000.
[25] J.L. Roberts Jr., D.T. Sawyer, Voltammetric determination of carbon monoxide at gold electrodes, J. Electroanal. Chem. 7 (4) (1964) 315–319.
[26] P. Rodríguez, A.A. Koverga, M.T.M. Koper, Carbon monoxide as a promoter for its own oxidation on a gold electrode, Angew. Chem. Int. Ed. 49 (7) (2010) 1241–1243.
[27] P. Rodriguez, N. Garcia-Araez, M.T.M. Koper, Self-promotion mechanism for CO electrooxidation on gold, Phys. Chem. Chem. Phys. 12 (32) (2010) 9373–9380.
[28] B.B. Blizanac et al., Anion adsorption, CO oxidation, and oxygen reduction reaction on a Au(100) surface: the pH effect, J. Phys. Chem. B 108 (2) (2003) 625–634.
[29] S.-C. Chang, A. Hamelin, M.J. Weaver, Reactive and inhibiting adsorbates for the catalytic electrooxidation of carbon monoxide on gold (210) as characterized by surface infrared spectroscopy, Surf. Sci. 239 (3) (1990) L543–L547.
[30] B.B. Blizanac et al., Surface electrochemistry of CO on reconstructed gold single crystal surfaces studied by infrared reflection absorption spectroscopy and rotating disk electrode, J. Am. Chem. Soc. 126 (32) (2004) 10130–10141.

[31] P. Rodriguez, J.M. Feliu, M.T.M. Koper, Unusual adsorption state of carbon monoxide on single-crystalline gold electrodes in alkaline media, Electrochem. Commun. 11 (6) (2009) 1105–1108.

[32] H. Kita, H. Nakajima, K. Hayashi, Electrochemical oxidation of CO on Au in alkaline solution, J. Electroanal. Chem. Interfacial Electrochem. 190 (1–2) (1985) 141–156.

[33] S.C. Chang, A. Hamelin, M.J. Weaver, Dependence of the electrooxidation rates of carbon monoxide at gold on the surface crystallographic orientation: a combined kinetic-surface infrared spectroscopic study, J. Phys. Chem. 95 (14) (1991) 5560–5567.

[34] P. Rodriguez et al., CO electroxidation on gold in alkaline media: a combined electrochemical, spectroscopic, and DFT study, Langmuir 26 (14) (2010) 12425–12432.

[35] P. Rodriguez, Y. Kwon, M.T.M. Koper, The promoting effect of adsorbed carbon monoxide on the oxidation of alcohols on a gold catalyst, Nat. Chem. 4 (2012) 177–182.

[36] S. Guerin et al., A combinatorial approach to the study of particle size effects on supported electrocatalysts: oxygen reduction on gold, J. Comb. Chem. 8 (5) (2006) 679–686.

[37] B.E. Hayden, D. Pletcher, J.-P. Suchsland, Enhanced activity for electrocatalytic oxidation of carbon monoxide on titania-supported gold nanoparticles, Angew. Chem.—Int. Ed. 46 (19) (2007) 3530–3532.

[38] B.E. Hayden et al., CO oxidation on gold in acidic environments: particle size and substrate effects, J. Phys. Chem. C 111 (45) (2007) 17044–17051.

[39] S. Guerin et al., Combinatorial approach to the study of particle size effects in electrocatalysis: synthesis of supported gold nanoparticles, J. Comb. Chem. 8 (5) (2006) 791–798.

[40] M. Valden, X. Lai, D.W. Goodman, Onset of catalytic activity of gold clusters on titania with the appearance of nonmetallic properties, Science 281 (5383) (1998) 1647–1650.

[41] A. Moore et al., Insulating diamond particles as substrate for Pd electrocatalysts, Chem. Commun. 47 (27) (2011) 7656–7658.

[42] W. Hongthani, N.A. Fox, D.J. Fermin, Electrochemical properties of two dimensional assemblies of insulating diamond particles, Langmuir 27 (8) (2011) 5112–5118.

[43] A.I. Yanson et al., Cathodic corrosion: a quick, clean, and versatile method for the synthesis of metallic nanoparticles, Angew. Chem. Int. Ed. 50 (28) (2011) 6346–6350.

[44] P. Rodriguez et al., Cathodic corrosion as a facile and effective method to prepare clean metal alloy nanoparticles, J. Am. Chem. Soc. 133 (44) (2011) 17626–17629.

[45] C.J. Weststrate et al., CO adsorption on Au(3 1 0) and Au(3 2 1): 6-fold coordinated gold atoms, Surf. Sci. 603 (13) (2009) 2152–2157.

[46] T. Jiang et al., Trends in CO oxidation rates for metal nanoparticles and close-packed, stepped, and kinked surfaces, J. Phys. Chem. C 113 (24) (2009) 10548–10553.

[47] A. Hussain et al., DFT study of CO and NO adsorption on low index and stepped surfaces of gold, Surf. Sci. 603 (17) (2009) 2734–2741.

[48] S.A.C. Carabineiro, B.E. Nieuwenhuys, Adsorption of small molecules on gold single crystal surfaces, Gold Bull. 42 (4) (2009) 288–301.

[49] T.A. Baker, X.Y. Liu, C.M. Friend, The mystery of gold's chemical activity: local bonding, morphology and reactivity of atomic oxygen, Phys. Chem. Chem. Phys. 13 (1) (2011) 34–46.

[50] T.A. Baker, C.M. Friend, E. Kaxiras, Atomic oxygen adsorption on Au(1 1 1) surfaces with defects, J. Phys. Chem. C 113 (8) (2009) 3232–3238.

[51] T.V. Choudhary, D.W. Goodman, Catalytically active gold: the role of cluster morphology, Appl. Catal. A 291 (1–2) (2005) 32–36.

[52] M. Mavrikakis, P. Stoltze, J.K. Norskov, Making gold less noble, Catal. Lett. 64 (2–4) (2000) 101–106.

[53] M. Arenz, U. Landman, U. Heiz, CO combustion on supported gold clusters, Chemphyschem: Eur. J. Chem. Phys. Phys. Chem. 7 (9) (2006) 1871–1879.

[54] N. Lopez et al., The adhesion and shape of nanosized Au particles in a Au/TiO2 catalyst, J. Catal. 225 (1) (2004) 86–94.

[55] A. Sanchez et al., When gold is not noble: nanoscale gold catalysts, J. Phys. Chem. A 103 (48) (1999) 9573–9578.

[56] V. Subramanian, E.E. Wolf, P.V. Kamat, Catalysis with TiO2/gold nanocomposites. Effect of metal particle size on the fermi level equilibration, J. Am. Chem. Soc. 126 (15) (2004) 4943–4950.

[57] Y. Yin et al., Scanning tunneling microscopy and in situ spectroscopy of ultra thin Ti films and nano sized TiOx dots induced by STM, Appl. Surf. Sci. 199 (1–4) (2002) 319–327.

[58] D. Matthey et al., Enhanced bonding of gold nanoparticles on oxidized TiO2(1 1 0), Science 315 (5819) (2007) 1692–1696.

[59] K. Lauwaet et al., Morphology and electronic properties of thermally stable TiOx nanoclusters on Au(1 1 1), Phys. Rev. B 83 (15) (2011) 155433.

[60] D. Dalacu, J.E. Klemberg-Sapieha, L. Martinu, Substrate and morphology effects on photoemission from core-levels in gold clusters, Surf. Sci. 472 (1–2) (2001) 33–40.

[61] Z.-Y. Yuan, J.-F. Colomer, B.-L. Su, Titanium oxide nanoribbons, Chem. Phys. Lett. 363 (3–4) (2002) 362–366.

[62] Y.-F. Chen et al., Preparing titanium oxide with various morphologies, Mater. Chem. Phys. 81 (1) (2003) 39–44.